Ernst Schering Foundation Symposium Proceedings, Vol. 4, pp. 153–187
DOI 10.1007/2789_2008_093

Published Online: 03 July 2008

Minimally Invasive Biomarkers for Therapy Monitoring

P. McSheehy(✉), P. Allegrini, S. Ametaby, M. Becquet, T. Ebenhan, M. Honer, S. Ferretti, H. Lane, P. Schubiger, C. Schnell, M. Stumm, J. Wood

Oncology Research, Novartis Pharma AG, 4002 Basel, Switzerland
email: *paul_mj.mcsheehy@novartis.com*

Abstract. Development of new drugs and optimal application of the drugs currently in use in clinical chemotherapy requires the application of biomarkers. Ideally, these biomarkers would stratify patients so that only those patients likely to respond to a particular therapy receive that therapy. However, that is not always feasible, and an alternative is to make use of early response biomarkers to determine the responding population. In this paper, a number of generic (i.e. not necessarily specific to the action mechanism of the compound) early-

response biomarkers are discussed and compared in different models and with three compounds with quite different mechanisms of action: a VEGF-R inhibitor (PTK787), an mTOR inhibitor (RAD001) and a microtubule stabiliser (EPO906). The methods include noninvasive DCE-MRI and PET imaging for measuring tumour vascularity, metabolism and proliferation, as well as the minimally invasive WIN method for measuring tumour interstitial pressure (IFP). The data show that drug-induced changes in IFP (ΔIFP) involve mechanism-dependent changes in the tumour vascular architecture, and that ΔIFP may be considered a universal generic early-response marker of tumour response to therapy.

1 Introduction

Chemotherapy remains a mainstay for the treatment of cancer, which until 10 years ago involved predominantly cytotoxics, including alkylating agents, anti-metabolites and agents acting against microtubules. More recently, targeted agents have been added to the arsenal such as trastuzumab (Herceptin), imatinib (Glivec) and bevacizumab (Avastin). The successful development of the new generation of targeted agents demands the application of biomarkers so that the patient population is stratified, i.e. the right people get the right drugs. In fact, suitable biomarkers would aid the application of all chemotherapies since in some cancer indications response rates do not predict progression-free survival (PFS) or overall survival (OS). Furthermore, biomarkers are important for determining the optimal biological dose of a new compound in Phase-I/II trials, since these newer agents may not cause rapid changes in tumour size and thus RECIST (response-evaluation criteria in solid tumours), which was developed for the cytotoxics, may no longer be appropriate. Finally, generic biomarkers, i.e. markers not necessarily specific to the drug in question, can also be useful for measuring an early response of the tumour, before a change in tumour size (if any) or as an alternative or indeed better surrogate for some later endpoints.

A number of these generic biomarkers are now being used in the clinic to aid drug development of both traditional cytotoxics and the targeted agents. The approaches include monitoring blood biomarkers such as PSA or CA-125 as well as imaging biomarkers such as dynamic contrast-enhanced magnetic resonance imaging (DCE-MRI),

positron-emission tomography using the glucose analogue ^{18}FDG (2′-[^{18}F]-fluoro-2′-deoxyglucose) or the thymidine analogue ^{18}FLT (3′-deoxy-3′-[^{18}F]-fluorothymidine) and the minimally invasive method of measuring tumour interstitial fluid pressure (IFP). Imaging methods are a powerful means of investigating fairly specific aspects of the tumour vasculature, metabolism and proliferation. Tumour IFP has for some time been identified as a parameter that in tumours is raised above normal tissue values, including human tumours in the clinic (Jain 1994), where it was identified as an independent prognostic indicator (Milosevic et al. 2001). Furthermore, recent clinical studies have shown that chemotherapy with bevacizumab (Willet et al. 2004) or paclitaxel (Taghian et al. 2005) can cause decreases in tumour IFP, which may be related to tumour response. Although the biological basis of a raised IFP is known to be related to a high vessel permeability, poor lymphatic drainage, poor perfusion and high cell density around the blood vessels as well as elevated glycolysis (Rutz 1999). The biology underlying a drug-induced change in IFP is less well studied.

The main aim of this paper was to focus on the three different early-response markers of MRI, PET and IFP and compare the response and biological data obtained for three different compounds currently in drug development, each with a different mechanism of action. In this way, the biological basis of a drug-induced change in IFP could be explored and the most appropriate early-response biomarker for each compound could be identified.

2 Methods

2.1 Compounds

Most studies utilised Novartis compounds synthesised in the Chemistry Department, Basel, Switzerland. This included the following compounds: NVP-AEE788, a dual inhibitor of VEGF-R and EGFR, EPO906 (generic name, patupilone), a microtubule stabiliser (MTS), PTK787 (generic name, vatalanib, aka PTK/ZK), a pan-VEGF-R inhibitor, RAD001 (generic name, everolimus), an mTOR inhibitor, STI571 (generic name, imatinib), a BCR-ABL, PDGF-R and c-Kit in-

hibitor, as well the alkylating agent cyclophosphamide (CP) and the anti-metabolite gemcitabine (Gemzar). Various pilot experiments were conducted to determine the optimal dose and schedule of the compounds to be used in vivo based upon achieving good anti-tumour efficacy and reasonable tolerability normally manifested as less than 15% body-weight loss.

Compounds were dosed daily (qd), weekly (qw) or two/three times per week (2qw, 3qw).

2.2 Animals

All animal studies conducted were in accordance with approved licenses as governed by the laws of the Kanton Basel.

2.2.1 Tumour Models

Human tumour xenografts were grown in Harlan nude mice (Novartis stock) following s.c. injection of cells in the animal flank. The human cell lines used were H-596 lung, HCT-116 colon, KB-31 cervical, HeLA cervical, U87MG glioma, 1A9 ovarian wild type and the paclitaxel-resistant form 1A9ptx10. In addition, two rat tumour xenografts in mice were created in the same way following s.c. injection of either C6 glioma or PROb colon cells. Tumour-bearing mice were used for efficacy, IFP and imaging studies once the tumour volume (TVol) was greater than 100 mm^3.

Syngeneic models used either rats or mice. The rat models were (a) A15 glioma and (b) PROb colon cells injected s.c. in the flank of BDIX rats and (c) BN472 breast tumour fragments implanted in the mammary fat-pad (orthotopic) of brown-Norway (BN) rats. Rats were normally in the range of 150–200 g body weight and tumours were used once the TVol was greater than 200 mm^3. The mouse models were (a) RIF-1 fibrosarcoma cells injected s.c. (effectively orthotopic) in the flank of C3H/He mice and (b) B16/BL6 melanoma cells injected under the skin (orthotopic) in the ear of C57/BL6 mice; the B16 tumours rapidly metastasise to the lymph nodes of the neck and the B16-mets were used for most studies. Both mouse models were used for studies after 10–14 days' growth. Mice were normally in the range of 20–25 g body

weight. Further details of the models are available in Rudin et al. (2005) and Ferretti et al. (2005).

2.3 Interstitial Fluid Pressure

Tumour interstitial fluid pressure (IFP) was measured using the wick-in-needle (WIN) method in which a standard 23-gauge needle connected to a pressure transducer was inserted into the central part of the tumours, and the pressure monitored for a period of 10 min in animals anaesthetised with 2.5% isoflurane delivered at 2 l/min. (Ferretti et al. 2005).

2.4 Magnetic Resonance Imaging

Magnetic resonance imaging (MRI) was performed on both mouse B16/BL6 lymph-node metastases and rat BN472 mammary tumours. For all studies, animals were anaesthetised using 1.5% isoflurane in a 1:2 v/v mixture of O_2/N_2O and placed on an electrically warmed pad for cannulation of one of the tail-veins using a 30-guage needle attached to an infusion line of 30 cm and volume 80 μl to permit remote administration of the contrast agent. The animals were positioned on a cradle in a supine position inside the 30 cm horizontal bore magnet and the body temperature was maintained at 37±1°C using a warm air flow and was monitored with a rectal probe. MRI experiments were performed on a Bruker DBX 47/30 spectrometer at 4.7 T equipped with a self-shielded 12-cm bore gradient system, as previously described (Rudin et al. 2005).

2.4.1 Dynamic Contrast-Enhanced MRI

The low-molecular-weight (MW) contrast agent GdDOTA (gadolinium tetra-azocyclododecane-tetra-acetate, Dotarem®) was injected (0.1 mmol/kg) to determine tumour vascular permeability (initial slope of GdDOTA uptake, VP) and extravasion, i.e. tumour extracellular leakage space (final value for GdDOTA uptake, LS) and the first 20 points (102 s) from the injection of GdDOTA were used to calculate the initial area under the enhancement curve for the contrast agent (iAEUC). A similar approach was taken in some experiments using the high-

MW (>1 kD) contrast agent, Vistarem (P792, a dendrimeric Gd-based macromolecular contrast agent), which was injected at 200 µl/100 g body weight. Using an average arterial input function, K^{trans} estimates were obtained from a nonlinear regression analysis of the signal enhancement curves after Vistarem administration.

In some experiments, the iron oxide particle intravascular contrast agent, Endorem®, was injected (6 mmol/kg of iron) 15–30 min after the other contrast agent, to determine the tumour relative blood volume (rBVol), and the initial slope of uptake of Endorem by the tumour was used as a blood flow index (BFI). The principles behind measurement of these parameters have already been fully described (Rudin et al. 2005).

2.4.2 Dynamic Susceptibility Contrast MRI

In rats bearing BN472 tumours, the contrast agent Sinerem, which is an iron oxide particle intravascular contrast agent, was injected i.v. (0.2 mmol/kg iron) for measurement of tumour vessel size and absolute tumour blood volume as a percentage of the total tumour size (aBVol). Briefly, the method is based on the measurement ΔR_2 and ΔR_2* relaxation rate constants induced by the injection of an intravascular slow-clearance superparamagnetic contrast agent. Based on relaxation theory, it was shown in vivo that the ΔR_2*/ΔR_2 ratio is related to the diameter of the vessels (Tropres et al. 2001).

2.5 Positron Emission Tomography

All experiments were conducted at the ETH as previously described (McSheehy et al. 2007). Briefly, a quad-HIDAC tomograph with a camera and four detector banks, each comprising four high-density avalanche chamber (HIDAC) modules, was used. The field of view was 280 mm axially and 170 mm in diameter, allowing the acquisition of whole-body images in a single bed position. Animals were anaesthetised with isoflurane in an air/oxygen mixture 20 min after injection of a maximum of 200 µl of the radiotracer ^{18}FDG (15–25 MBq per mouse) or ^{18}FLT (5–15 MBq per mouse) via a lateral tail vein. Acquisition of PET data was initiated 30 min after injection and lasted for 20–30 min. Data were acquired in list mode and reconstructed in a single time frame us-

ing the OPL-EM algorithm with a bin size of 0.5 mm, a matrix size of 160×160×200 and a resolution recovery width of 1.3 mm. Reconstruction did not include scatter, random and attenuation correction.

Image files were evaluated by region-of-interest (ROI) analysis using the dedicated software Pmod. This provided total activity concentrations in the tumour (counts/ml), which were normalised to the injected dose per body weight (kBq/g) to give a unitless normalised uptake value (NUV).

2.6 Histology and Immunohistochemistry

At the endpoint of some experiments following efficacy, IFP or imaging studies, the nuclear staining dye, H33342, was injected i.v. at 20 mg/kg (2 mg/ml in normal saline) into anaesthetised animals and after 45 s, the animals were sacrificed by cervical dislocation and the tumour removed. The tumour was sliced through the central plain and analyzed using a magnification of 100x to determine the blood vessel width and blood vessel density (Rudin et al. 2005).

In other experiments, nothing was injected and tumour slices were harvested from the largest circumference of the tumour and fixed in 4% phosphate buffered formaldehyde for 24 h at 4°C and processed into paraffin before preparation and staining by (a) haematoxylin and eosin (H&E) for evaluation of necrosis, (b) caspase-3 to measure apoptosis and (c) Ki67 to measure proliferation, as previously described (Ferretti et al. 2005).

2.7 Data Analysis

2.7.1 Efficacy and Tolerability

Body weight, BW (g) and tumour volume (TVol) were measured three times per week. Efficacy was assessed as the T/C from the change (difference) in TVol using the endpoint (at 1–3 weeks after treatment initiation) to give a T/C_{TVol}. In a similar manner, the effect of the drug on BW was also quantified to give the fractional change in BW (ΔBW), i.e. BW_{after}/BW_{before}, for both vehicle-control and drug-treated groups so that the $T/C_{BW} = \Delta BW_{(treated)}/\Delta BW_{(control)}$.

2.7.2 Biomarkers: IFP, MR, PET and IHC

Individual values for each tumour at each different time point from before treatment (day 0) and after treatment (1–10 days after treatment initiation) are presented. Alternatively, or in addition, the fractional change (ΔF) in the parameter (final value/starting value) for each tumour at each time point after treatment is also presented from which the T/C for that parameter may be determined as described for BW, e.g. T/C_{IFP} or T/C_{BVol} or T/C_{FLT} etc.

2.7.3 Statistics

Differences between the means of TVol and BW of vehicle or compound-treated animals were assessed using a two-tailed *t*-test or one-way ANOVA, as required. If the normality and/or the equal variance test failed, a logarithmic transformation was applied; however, this did not always normalise the data.

For the biomarker analysis, data was examined in two different ways: (a) using the raw values and a two-way repeated measures analysis of variance (2W-RM-ANOVA) with Tukey post-hoc and (b) comparing the differences in fractional changes of the mean values induced by treatments using a one-way ANOVA with Tukey-test post-hoc or a two-tailed *t* -test, as appropriate.

All data are shown as mean±SEM except where stated to be ±SD, with the significance value set at $p < 0.05$. In all the figures, significance is represented as follows: * $p < 0.05$, ** $p < 0.01$, *** $p < 0.001$.

3 Results

3.1 Tumour IFP

We evaluated basal tumour IFP (mm Hg) in ten different experimental tumour models, including human tumours in nude mice as well as syngeneic models in mice and rats (Table 1). The highest mean IFPs were all associated with rat tumours, whether grown in mice or rats s.c. or orthotopically. However, rat colon PROb tumours implanted s.c. (ectopically) in rats exhibited an IFP of 15.2±0.7 mm Hg, ($n = 45$), whereas the

Table 1 Basal tumour IFP in different experimental models

Tumour	Histotype	Species	Host, Strain	Type	*n*	IFP
PROb	Colon	Rat	Rat, BDIX	S.c.	45	15.2 ± 4.7
C6	Glioma	Rat	Nude mouse, Harlan	S.c.	36	14.6 ± 9.0
C6	Glioma	Rat	Nude mouse, Balb/c	S.c.	35	13.7 ± 9.5
BN472	Breast	Rat	Rat, BN	S.c.	12	13.1 ± 5.4
BN472	Breast	Rat	Rat, BN	Ortho	218	12.3 ± 4.4
HeLa	Cervical	Human	Nude mouse, Harlan	S.c.	15	11.2 ± 5.8
PROb	Colon	Rat	Nude mouse, Harlan	S.c.	14	10.5 ± 8.6
1A9	Ovarian	Human	Nude mouse, Harlan	S.c.	62	7.2 ± 4.7
1A9ptx10	Ovarian	Human	Nude mouse, Harlan	S.c.	65	6.2 ± 4.0
B16/BL6	Melanoma	Mouse	Mouse, C57/BL6	Ortho	35	6.7 ± 3.0
B16/BL6	Melanoma	Mouse	Mouse, C57/BL6	S.c.	14	6.3 ± 3.3
RIF-1	Fibrosarc	Mouse	Mouse, C3H/He	S.c./orth	29	6.3 ± 3.2
U87MG	Glioma	Human	Nude mouse, Harlan	S.c.	24	4.4 ± 3.4

The results show the mean ± SD IFP in mmHg. Tumours were implanted either ectopically (s.c.) or orthotopically (ortho)

same tumour also implanted s.c. in the flank of nude mice had a significantly ($p = 0.01$) lower IFP (10.5±2.3 mm Hg, $n = 14$). This observation emphasises the important role of the host in the growth of a tumour and thus also the basal IFP of that tumour. In contrast, the IFP of C6 tumours was not significantly altered when grown s.c. in two different types of nude mouse (Harlan or Balb/c). Furthermore, in two syngeneic orthotopic models (BN472 in rats and B16/BL6 in mice), there was no evidence that the implantation site was important (Table 1). In the BN472 and B16 models, tumours were in some cases grown both s.c. and orthotopically in the same animal allowing a paired comparison which

Table 2 Examples of the effect of different compound treatments on tumour IFP in different tumour models

Compound	Dose and schedule	Day 2/3		Day 6/7	
		T/C_{TVol}	T/C_{IFP}	T/C_{TVol}	T/C_{IFP}
	BN472 rat breast model				
AEE788	60 mg/kg, 3 qw	0.44	0.48*	0.48*	0.49
PTK787	200 mg/kg, qd	0.47	0.66	0.3	0.5*
RAD001	5 mg/kg, 3 qw	0.96	0.74	0.75	0.62*
EPO906	1.5 mg/kg, once	0.36	0.52*	0.06*	0.32*
STI571	100 mg/kg, 2 qd	0.04*	0.75*	–	–
CP	50 mg/kg, qw	0.01*	0.82	−0.2*	0.65*
Gemzar	150 mg/kg, qw	0.07	0.51*	0.07*	1.18
	1A9 human ovarian model				
EPO906	4 mg/kg, once	0.30	0.47*	0.14*	0.18*
	PROb rat colon model				
STI571	200 mg/kg, qd	0.54	0.59*	–	–

The results show the drug-induced change TVol (*efficacy*) and the IFP in a one or two (*pooled*) experiments ($n = 6$–21) with respect to vehicle-treated animals as the respective T/C (see Methods), where *indicates a significant difference ($p < 0.05$) to vehicle

showed no significant difference and thus indicating that implantation-site had no effect on IFP ($P < 0.7$). In general, most human tumour s.c. xenografts had rather low IFPs and in some cases (e.g. U87MG), there were several tumours that were almost unmeasurable (<2.0 mm Hg). One other paired comparison was possible: human ovarian tumours 1A9 (wild type) and the paclitaxel-resistant tumour (1A9ptx10), which has

mutations in the drug's molecular target of β-tubulin; here there was also no significant difference in IFP.

3.1.1 Effect of Different Compounds on Tumour IFP

All compounds tested, independent of the tumour type and their mechanism of action, reduced tumour IFP significantly either fairly rapidly (after 2–3 days) or after 1 week (Table 2). The largest decreases in IFP were associated with the microtubule inhibitor EPO906, typically greater than 70% decreases in IFP at maximal doses, and an example of a longitudinal experiment in the RIF-1 model with EPO906 is shown in Fig. 1. For all compounds tested, the decrease in IFP was dose-dependent and there was a plateau in the maximum decrease achievable. Significant decreases in tumour IFP only occurred when there was a significant decrease in tumour volume (TVol) caused by compound treatment. This suggested there was a relationship between decreases in IFP and the effectiveness of anti-tumour efficacy. In fact, highly significant positive correlations could be shown between early (day 2/3) decreases in IFP (expressed as the fractional change for each tumour, ΔIFP) and the eventual change (i.e. ΔTVol) of that tumour (see Fig. 2). Again, the strength of the correlation was independent of the mechanism of action of the compound, with the targeted agents PTK787, EPO906 and gemcitabine all showing similar r-values (0.61–0.68; $p < 0.01$). However, these correlations were only significant when the studies were done on orthotopic tumours (BN472, RIF-1); other studies using the 1A9ptx10, PROb, HeLa or the U87MG models failed to reach significance except for 1A9wt, but then only after 7 days (Table 3).

3.1.2 Basal IFP and Compound Response

In general, the basal IFP of tumours showed no correlation with the outcome of tumour therapy. In part this may reflect that experimental tumour models are designed to show minimal heterogeneity and also that many of the studies from one dose were relatively small even when pooling different experiments. Nevertheless, in two cases in the BN472 model, PTK787 ($n = 19$) and EPO906 ($n = 11$) showed trends for a significant ($p = 0.04$ to 0.07) negative correlation between the basal IFP and

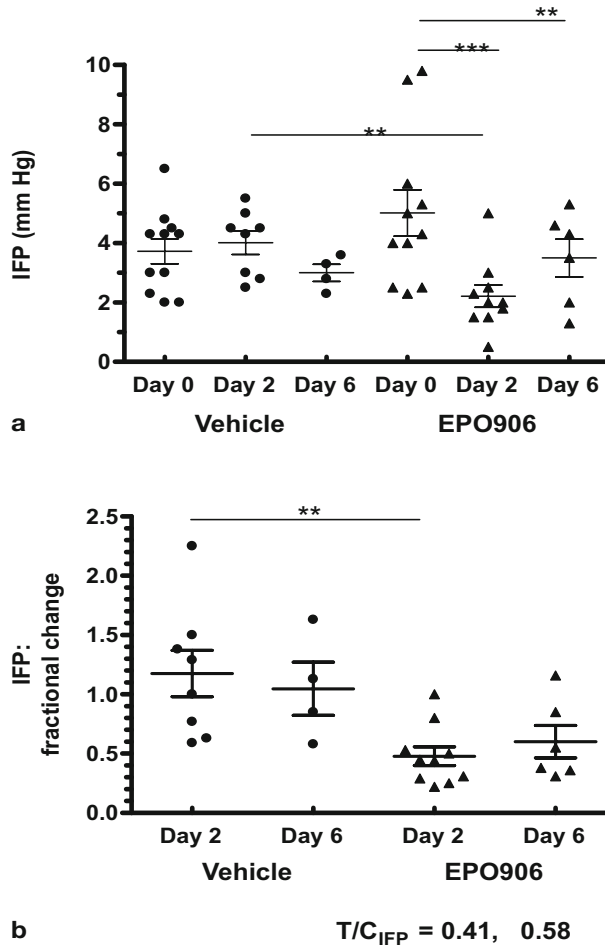

Fig. 1a,b. Longitudinal effect of EPO906 on the IFP of RIF-1 tumours. C3H mice bearing RIF-1 tumours were treated with EPO906 (5 mg/kg i.v.) or vehicle once on day 0 and tumour IFP measured using the WIN method. The results show (**a**) IFP values for individual tumours and associated mean±SEM on respective days (significance assessed using a 2W-RM-ANOVA), (**b**) individual fractional changes in IFP and associated mean±SEM relative to baseline measurements (significance assessed using a two-tailed *t*-test)

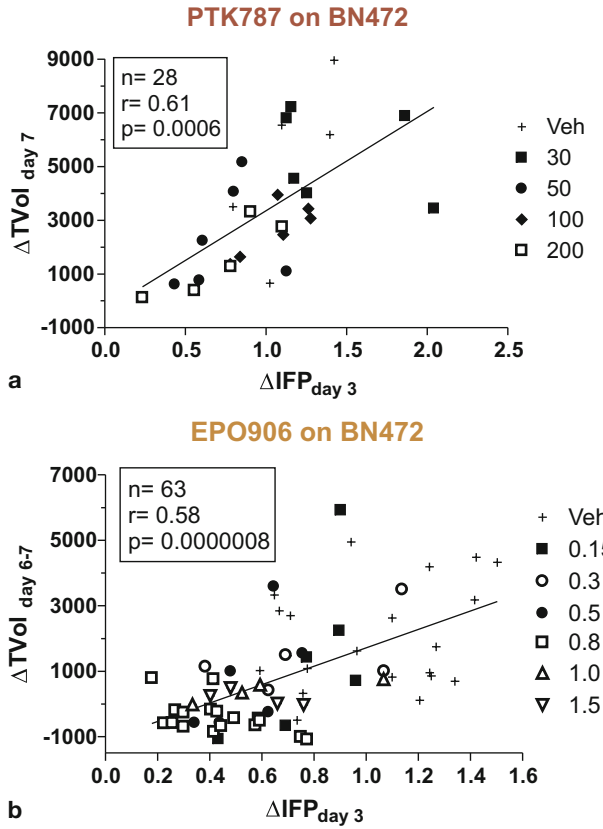

Fig. 2a,b. Correlation between fractional change in IFP and efficacy. The results show the compound-induced fractional change in IFP (ΔIFP) 2–3 days after treatment initiation and the tumour volume change (ΔTVol) after 6–7 days for individual tumours treated with different compound doses (mg/kg) shown on the *right-hand side* of the graphs. PTK787 treatment was daily, EPO906 and Gemzar weekly (q.w.) or twice weekly (2 q.w.)

TVol on day 7 (Fig. 3). Since a smaller change in TVol reflects a better response, this data implies that tumours with a higher IFP may actually

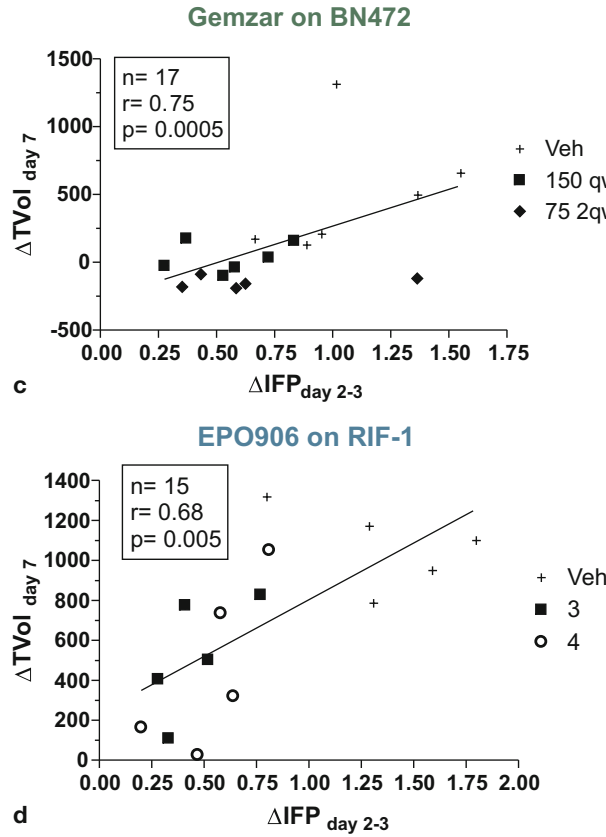

Fig. 2c,d. Correlation between fractional change in IFP and efficacy. The results show the compound-induced fractional change in IFP (ΔIFP) 2–3 days after treatment initiation and the tumour volume change (ΔTVol) after 6–7 days for individual tumours treated with different compound doses (mg/kg) shown on the *right-hand side* of the graphs. PTK787 treatment was daily, EPO906 and Gemzar weekly (q.w.) or twice weekly (2 q.w.)

be expected to respond better to drug treatment, and thus measurement of the basal IFP of tumours might also aid patient stratification.

Table 3 Summary of correlations between compound-induced fractional changes in IFP and efficacy

Tumour model	Host	Drug	$\Delta IFP_{day\ 2\text{-}3}$ vs $\Delta TVol_{day\ 6\text{-}7}$			$\Delta IFP_{day\ 6\text{-}7}$ vs $\Delta TVol_{day\ 6\text{-}7}$		
			n	*r*	*P*	*n*	*r*	*P*
PROb	Nude mice	STI571	14	0.30	0.30	14	0.32	0.26
PROb	BDIX rat	STI571	12	0.22	0.49	12	0.27	0.40
BN472	*BN rat*	*AEE788*	*26*	*0.11*	*0.60*	*26*	*0.07*	*0.72*
BN472	*BN rat*	*PTK787*	*28*	***0.61***	***0.0006***	*28*	***0.64***	***0.0002***
BN472	*BN rat*	*RAD001*	*14*	*0.09*	*0.77*	*14*	*0.30*	*0.30*
1A9	Nude mice	EPO906	50	0.19	0.19	50	**0.31**	**0.005**
1A9ptx10	Nude mice	EPO906	58	0.23	0.08	58	0.11	0.40
U87MG	Nude mice	EPO906	22	0.04	0.85	22	0.02	0.95
HELA	Nude mice	EPO906	15	0.26	0.35	15	0.03	0.92
RIF-1	*C3H/He mice*	*EPO906*	*14*	***0.68***	***0.005***	*14*	*0.30*	*0.28*
BN472	*BN rat*	*EPO906*	*64*	***0.48***	***0.00005***	*64*	***0.43***	***0.0004***
RIF-1	*C3H/He mice*	*CP*	*11*	*0.33*	*0.32*	*11*	*0.19*	*0.58*
BN472	*BN rat*	*CP*	*16*	*0.36*	*0.17*	*16*	***0.64***	***0.008***
BN472	*BN rat*	*Gemzar*	*17*	***0.75***	***0.0005***	*17*	*0.03*	*0.92*

The results show the Pearson correlation coefficient, *r*, and the associated *p*-value. Values in **bold** indicate significant relationships; italic indicates orthotopic models

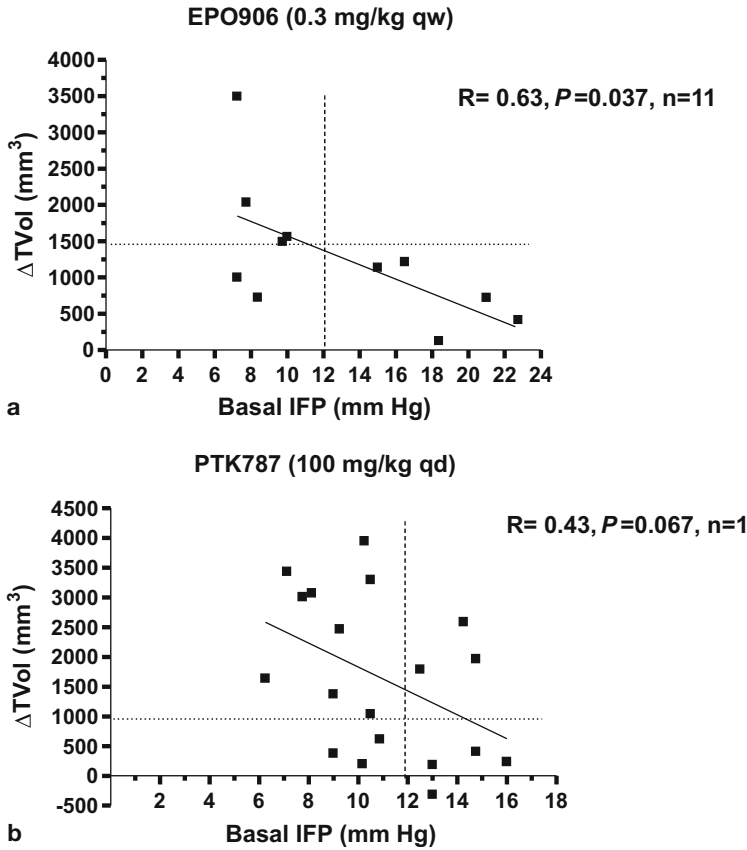

Fig. 3a,b. Correlation between basal IFP and efficacy. The results show individual BN472 tumour IFP values before treatment and correlation with the eventual change in TVol after 7 days for (**a**) EPO906 (**b**) PTK787

Fig. 4a,b. Longitudinal effect of EPO906 on the IFP and BVol of BN472 tumours. Rats bearing BN472 tumours were treated with EPO906 (0.8 mg/kg i.v.) or vehicle once on day 0 and tumour IFP and aBVol were measured as described in Methods. The results show the individual fractional changes in IFP and aBVol relative to baseline measurements (significance assessed using a two-tailed *t*-test)

3.2 Tumour IFP and MR-Measured Vascular Parameters

3.2.1 Comparison of Effects of EPO906 and PTK787

The effects of these two compounds on tumour growth, IFP and MR-measured vascular parameters were investigated in two different mod-

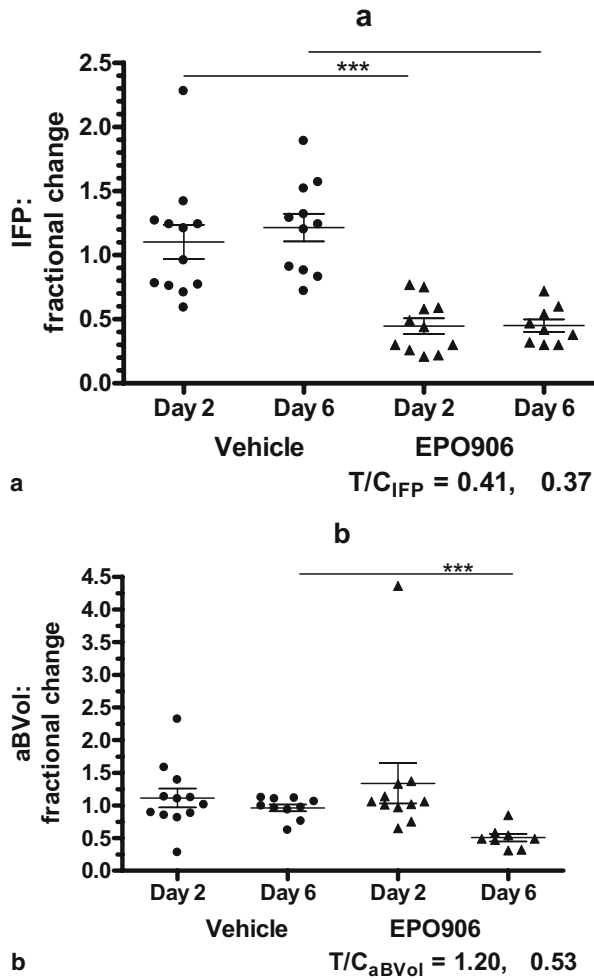

els. In the murine B16/BL6 orthotopic melanoma model, both compounds at optimal tolerable doses were able to significantly reduce tumour growth and caused significant decreases in IFP 2–4 days after treatment initiation. For EPO906, this was paralleled by a significant decrease in tumour blood volume (rBVol), with no change in blood vessel permeability (VP), intracellular leakage space (LS) or the composite parameter of iAUEC for the contrast agent Dotarem (Ferretti et al. 2005). For PTK787, VP and especially LS and iAUEC were reduced while the intravascular contrast agent, Endorem, showed that tumour blood flow (BFI) increased and BVol was not significantly affected (Rudin et al. 2005; Lee et al. 2006). To a certain extent, these results were consistent with the known mechanism of action of the two compounds; this will be discussed further below. However, IFP and the MRI-measured vascular parameters were not determined in the same animals, so the relationship of these parameters was not clear.

The effects of both PTK787 and EPO906 were investigated more extensively using the rat syngeneic orthotopic model of BN472 breast tumours.

EPO906 (0.8 mg/kg i.v. once) decreased significantly both IFP and BVol (Fig. 4a, b) and also tended to reduce the mean vessel size by day 6 ($T/C = 0.37$, $p = 0.15$). After 6 days, there was a significant inhibition of tumour growth, actually regression ($T/C_{TVol} = -0.3$), and histological analysis ex vivo demonstrated a 2.4-fold increase in apoptosis with respect to vehicle-treated rats but no change in necrosis. IFP and aBVol were strongly positively correlated with each other on day 6, and also with apoptosis and TVol (Fig. 5). Other experiments (data not shown) showed that the epothilone could significantly increase apoptosis in the BN472 tumour model and RIF-1 tumours after just 2 days of treatment. Thus, although both BVol and apoptosis were strongly correlated with IFP on day 6, the changes in BVol were slower than those in IFP, suggesting that at least at early time points, decreases in IFP may reflect more tumour cell death than destruction of the vasculature. Finally, further experiments in this model using either Dotarem or the higher-MW contrast agent Vistarem also failed to demonstrate significant decreases in K^{trans} either at day 2 or day 7 (maximum $T/C_{Ktrans} = 0.9$ and 0.8, respectively with Vistarem), confirming the lack of effect of EPO906 on vascular permeability observed in the B16/BL6 model.

In the BN472 model, PTK787 (100 mg/kg p.o. daily) significantly decreased tumour IFP by 25% and increased BFI by 40% after 3 days of treatment (Fig. 6a, b). However, changes were rather variable and significant changes could not be detected in blood vessel permeability, although there were strong trends indicating a decrease in leakage space and the composite parameter of iAUEC, as well as vessel width and rBVol (data not shown). Histological analysis also tended to show a decrease in the mean blood vessel width from 20.8±1.3 μm ($n = 14$) to 17.7±1.0 μm ($n = 15$) ($p = 0.068$) but not blood vessel density (14–16 vessels/mm^2). In the experiments where both IFP and MR

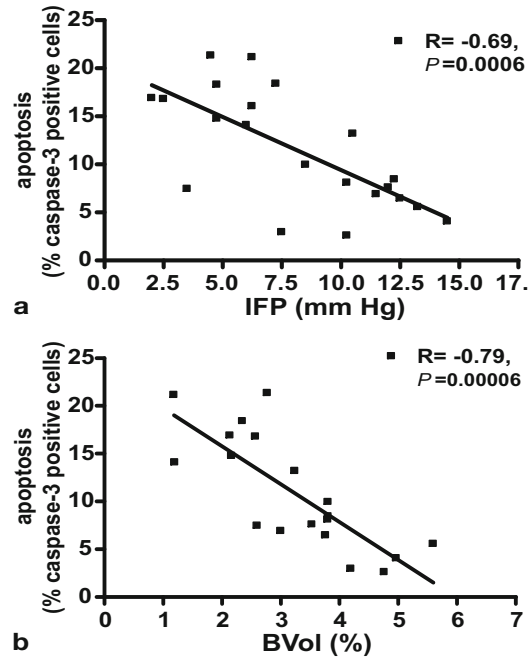

Fig. 5a,b. Correlations between IFP, aBVol, TVol and apoptosis in BN472 tumours following EPO906 treatment. Rats bearing BN472 tumours were treated with EPO906 (0.8 mg/kg); apoptosis, IFP, aBVol and TVol were measured on day 6. Data show the Pearson correlation coefficient and associated *p*-value

parameters were measured in the same rat tumour, there was a significant correlation between the pretreatment IFP and the BVol and BFI ($r = 0.45$, $p < 0.05$). Furthermore, as for EPO906, the change in IFP correlated with the change in BVol ($r = 0.71$, $p < 0.01$), although this did not reach significance for IFP and BFI. Thus, decreases in IFP in the BN472 tumour induced by PTK787 were associated with increased blood flow and narrower blood vessels rather than decreased blood volume and narrower blood vessels as for EPO906. The effects on tumour blood flow may have masked the decrease in vascular permeability that PTK787 would be expected to cause, since transfer of the low-MW contrast agent, Dotarem (GdDTPA), across the vasculature is influenced by both permeability and flow. Indeed, subsequent ex-

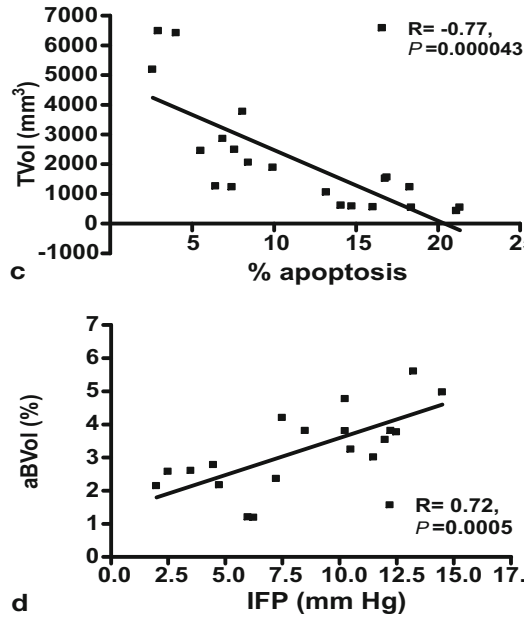

Fig. 5c,d. Correlations between IFP, aBVol, TVol and apoptosis in BN472 tumours following EPO906 treatment. Rats bearing BN472 tumours were treated with EPO906 (0.8 mg/kg); apoptosis, IFP, aBVol and TVol were measured on day 6. Data show the Pearson correlation coefficient and associated *p*-value

periments using a higher-MW contrast agent (Vistarem) in the BN472 model were able to demonstrate marked ($T/C_{Ktrans} = 0.37$) and highly significant ($p < 0.01$) decreases in the vascular transfer constant, K^{trans} after only 2 days of treatment (Schnell et al. 2008).

3.2.2 Effects of RAD001 on MR-Measured Parameters

RAD001 at 10 mg/kg p.o. daily was an effective inhibitor of growth, if not highly potent, of both B16/BL6 and BN472 tumours, leading to T/C_{TVol} of 0.5 and 0.63, respectively. As discussed above, RAD001 also caused a significant decrease in the IFP of BN472 tumours, but this was a late (day 7) rather than early effect (day 2/3). The effect of RAD001 on the IFP of B16/BL6 tumours was not investigated. RAD001 did not significantly affect any MR-measured vascular parameter after 2–3 days of treatment in either tumour model. There was a trend for the iAUEC (Dotarem or Vistarem) and K^{trans} (Vistarem) to increase, and in one experiment in B16/BL6 tumours, K^{trans} was significantly increased relative to vehicle ($T/C_{Ktrans} = 2.3$) after 6 days, while BVol tended to decrease and BFI to increase. No experiments were conducted in which both IFP and MR-measured vascular parameters were determined. Nevertheless, the data for RAD001 suggest that decreases in IFP were slow, but as for PTK787, eventually reflected increases in tumour blood flow manifested as a raised BFI and K^{trans}.

3.2.3 IFP and Tumour Vasculature: Conclusions

The data presented support the concept of a relationship between tumour IFP and tumour blood flow, permeability and blood volume. Although all compounds tested could reduce IFP either rapidly or after several days, the underlying reasons for the change in IFP depend upon the nature of the compound's mechanism of action. Thus, the classic anti-angiogenic agent, PTK787, which interferes with VEGF-R signalling on endothelial cells, reduced K^{trans}, narrowed the blood vessels and increased blood flow, events consistent with a normalisation of the tumour vasculature. The mTOR inhibitor RAD001, which inhibits both tumour cell and endothelial cell proliferation, slowly increased K^{trans} and blood flow. The MTS, EPO906, did not affect vascular permeabil-

ity, but did rapidly reduce blood volume, consistent with a strong anti-vascular effect.

3.3 Effects of Compounds on FDG and FLT-PET

3.3.1 In vivo Tumour Uptake of ^{18}FDG

Uptake and retention of the glucose analogue, ^{18}FDG, is considered to reflect both tumour cell glycolysis and cell viability but may also be influenced by other nonspecific factors including blood flow and infiltration by inflammatory cells such as macrophages (Mankoff et al. 2003). Indeed, our FDG-PET studies have shown that in the poorly vascularised s.c. xenograft models, the FDG signal is rim-limited while in well-vascularised orthotopic models (BN472, B16/BL6, RIF-1 and others) the signal is more homogeneous across the tumour.

PTK787 dosed at 100 mg/kg p.o. daily, failed to significantly affect FDG uptake by BN472 tumours after either 2 or 7 days of treatment (Fig. 7a, b).

In contrast, EPO906 (0.8 mg/kg i.v. once) in the same model, significantly reduced the FDG NUV at both time points, with the greatest effect being apparent after just 2 days, after which there was some recovery (Fig. 7c, d).

RAD001 (10 mg/kg p.o. daily) was tested in several different mouse models using either human tumour xenografts implanted in nude mice or the syngeneic orthotopic B16/BL6 model (McSheehy et al. 2007). The models used could be divided into two types based upon their sensitivity to inhibition of proliferation by RAD001 in vitro, i.e. the IC50. Thus, the human lung H-596 and murine melanoma B16/BL6 models had low IC50s of 5 nM and 0.7 nM, respectively, while the human cervical KB-31 and human colon HCT-116 had high IC50s of 1.8 and

Fig. 6a,b. Effect of PTK787 on the IFP and BFI of BN472 tumours. Rats bearing BN472 tumours were treated with PTK787 (100 mg/kg p.o. daily) or vehicle; tumour IFP and BFI were measured as described in methods on day 0 and day 3. The results show the individual fractional changes in IFP and BFI relative to baseline measurements (significance assessed using a two-tailed *t*-test)

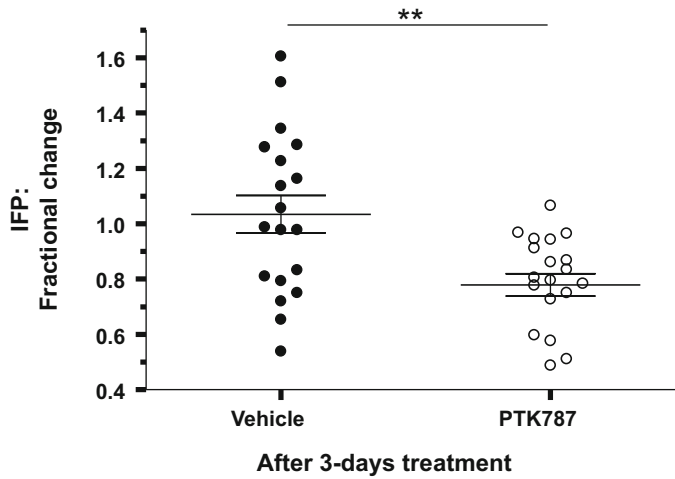

a $T/C_{IFP} = 0.75$

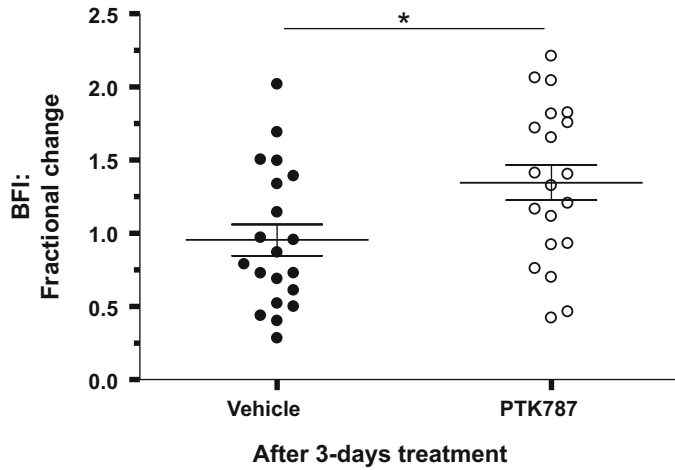

b $T/C_{BFI} = 1.42$

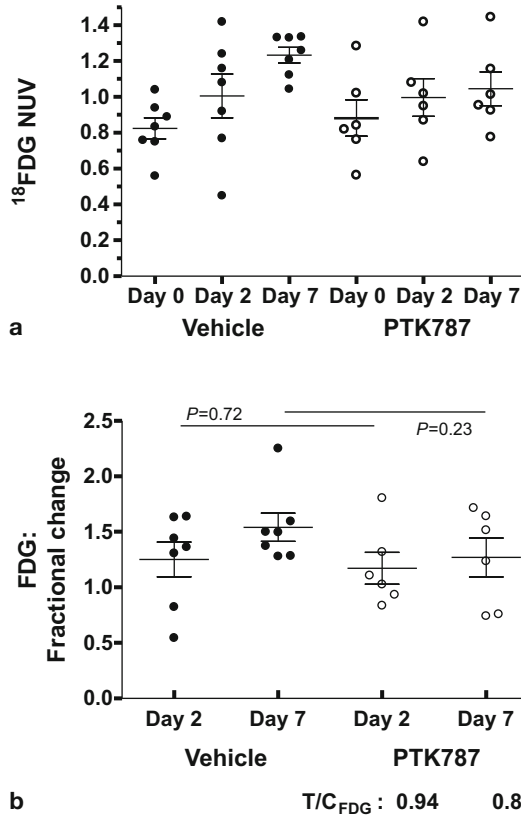

Fig. 7a,b. Effect of PTK787 or EPO906 on FDG uptake by BN472 tumours. Rats bearing BN472 tumours were treated with PTK787 (100 mg/kg p.o. daily) or EPO906 (0.8 mg/kg once) and the FDG uptake semi-quantified as the normalised uptake value (*NUV*) measured on days 0, 2, 6 or 7. The results show the values for individual tumours (a,c) and associated mean±SEM on respective days (significance assessed using a 2W-RM-ANOVA) and individual fractional changes (b,d) and associated mean±SEM relative to baseline measurements (significance assessed using a two-tailed *t*-test)

4.2 μM, respectively. A single oral dose of RAD001 leads to a Cmax in tumour-bearing mice of approximately 100 nM with a half-life in

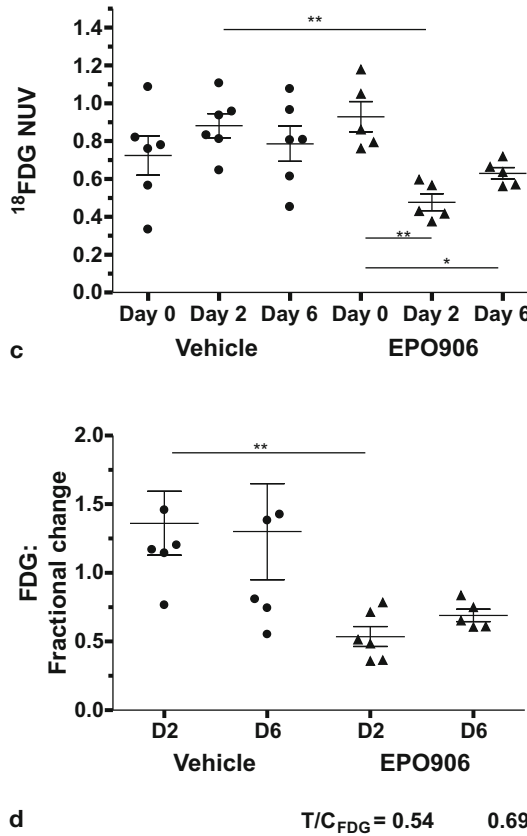

Fig. 7c,d. Effect of PTK787 or EPO906 on FDG uptake by BN472 tumours. Rats bearing BN472 tumours were treated with PTK787 (100 mg/kg p.o. daily) or EPO906 (0.8 mg/kg) and the FDG uptake semi-quantified as the normalised uptake value (*NUV*) measured on days 0, 2, 6 or 7. The results show the values for individual tumours (a,c) and associated mean±SEM on respective days (significance assessed using a 2W-RM-ANOVA) and individual fractional changes (b,d) and associated mean±SEM relative to baseline measurements (significance assessed using a two-tailed *t*-test)

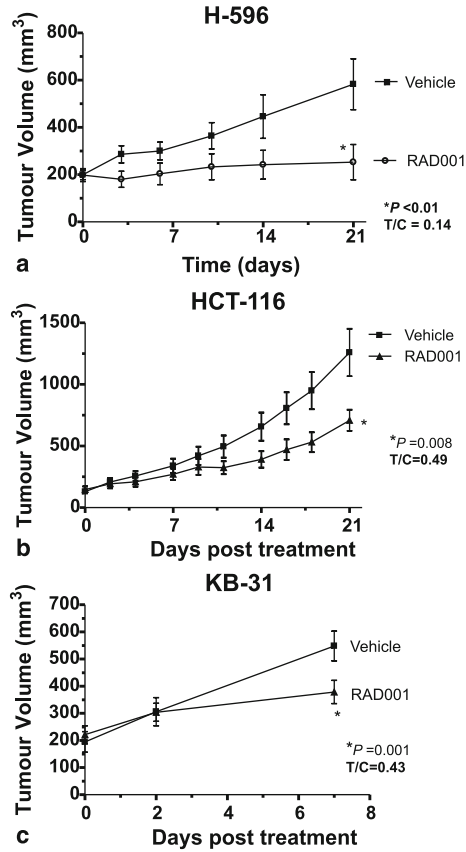

Fig. 8. Efficacy of RAD001 in different tumour models. Tumours were created as described in "Methods", and once they reached approximately 200 mm^3 they were treated daily with RAD001 (10 mg/kg p.o.). The results show the mean±SEM

the tumour and plasma of 8 and 16 h, respectively. Thus, the KB-31 and HCT-116 models would not be expected to respond to RAD001 in vivo, assuming the tumour cells were the only target. However, as Fig. 8 shows, after 1 week or more of treatment, significant inhibition

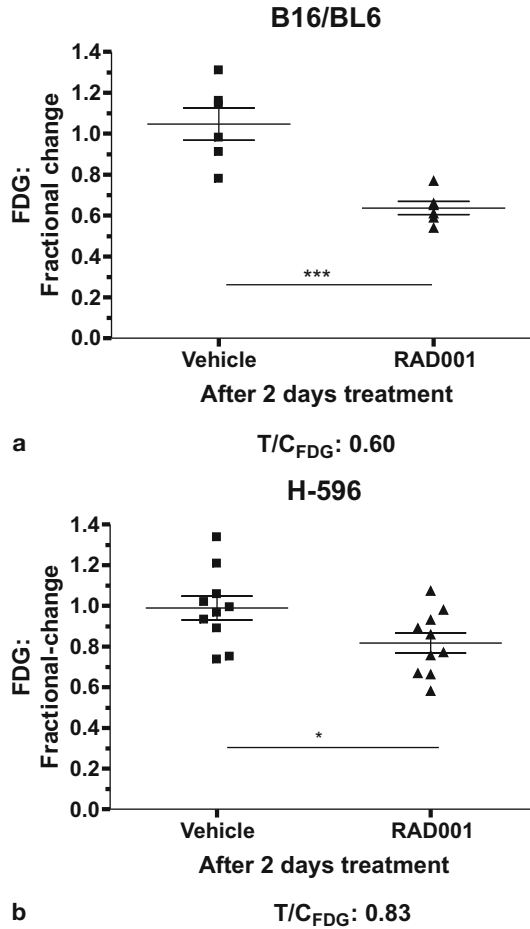

Fig. 9a,b. Effect of RAD001 on FDG uptake by different tumour models. The results show the fractional change in FDG-NUV after 2 or 7 days of daily treatment (10 mg/kg p.o. daily) and the associated T/C. The results show the values for individual tumours and associated mean±SEM on respective days (significance assessed using a 2W-RM-ANOVA) and individual fractional changes and associated mean±SEM relative to baseline measurements (significance assessed using a two-tailed *t*-test)

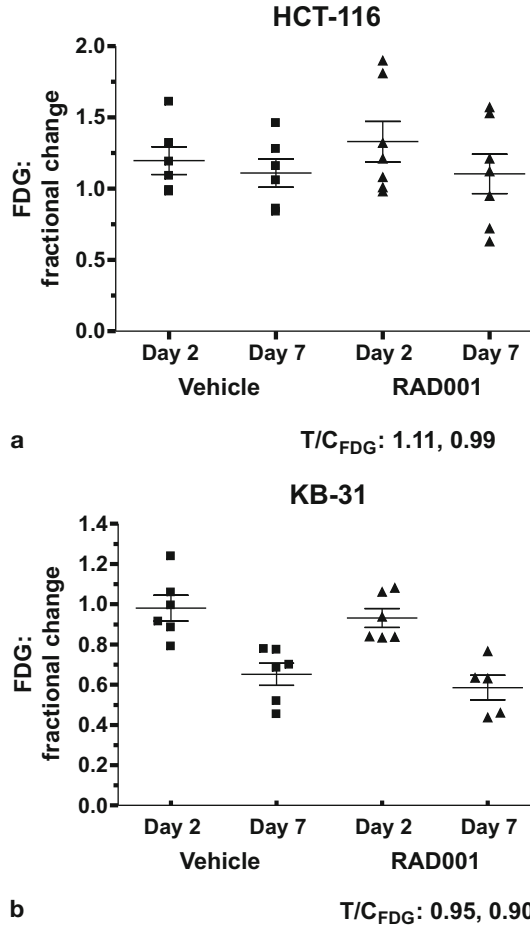

Fig. 9c,d. Effect of RAD001 on FDG uptake by different tumour models. The results show the fractional change in FDG-NUV after 2 or 7 days of daily treatment (10 mg/kg p.o. daily) and the associated T/C. The results show the values for individual tumours and associated mean±SEM on respective days (significance assessed using a 2W-RM-ANOVA) and individual fractional changes and associated mean±SEM relative to baseline measurements (significance assessed using a two-tailed *t*-test)

Fig. 10a–c. Effect of RAD001 on FLT uptake in two different tumour models and comparison with IHC measurements ex vivo. The results show the fractional change in FLT-NUV after 2–10 days daily treatment (10 mg/kg p.o. daily) and the associated T/C. In addition, for each model the IHC analysis of the Ki67 and apoptotic index is shown for each treatment group. For FLT, the results show the values for individual tumours and associated mean±SEM on respective days (significance assessed using a 2W-RM-ANOVA) and individual fractional changes and associated mean±SEM relative to baseline measurements (significance assessed using a two-tailed *t*-test). For IHC, the values for individual tumours and associated mean±SEM are shown for the respective endpoint

of growth, albeit modest, could be achieved, presumably reflecting the anti-angiogenic/anti-vascular activity of the compound. In confirmation of this hypothesis, significant ($p < 0.001$) decreases in blood vessel density were seen in the HCT-116 model: 4.8±0.5 vessels/mm^2 ($n = 10$), reduced to 2.6±0.6 vessels/mm^2 ($n = 10$) after 3 weeks of RAD001 treatment. Despite these growth-inhibitory effects, no significant changes in FDG NUV were apparent in either of the less sensitive models after 2–7 days of treatment, while in contrast, the more sensitive models showed significant decreases after just 2 days of treatment (Fig. 9).

3.3.2 In vivo Tumour Uptake of ^{18}FLT

EPO906 (5 mg/kg i.v. bolus) caused a rapid decrease in the FLT-NUV of murine RIF-1 tumours ($T/C_{FLT} = 0.78$) and this was associated, as expected, with a similar decrease in Ki67, which correlated significantly with the FLT-change after 24 h ($r = 0.42$, $p = 0.02$).

Daily RAD001 treatment (10 mg/kg p.o.) for 2 days caused a small but highly reproducible decrease in the ^{18}FLT-NUV of H-596 tumours ($T/C_{FLT} = 0.87$, 0.82, 0.80 for three independent experiments) but did not alter uptake in HCT-116 tumours even after 10 days of treatment (Fig. 10). IHC analysis showed that in neither of these models was there any significant change in apoptosis or Ki67.

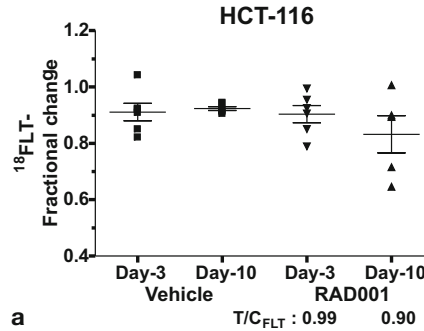
HCT-116
18FLT-Fractional change
1.2
1.0
0.8
0.6
0.4
Day-3
Day-10
Day-3
Day-10
Vehicle
RAD001
T/CFLT : 0.99
0.90

a

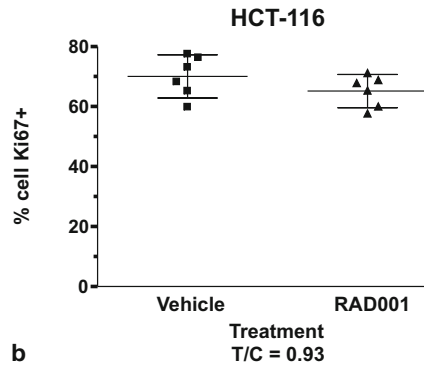
HCT-116
% cell Ki67+
80
60
40
20
0
Vehicle
RAD001
Treatment
T/C = 0.93

b

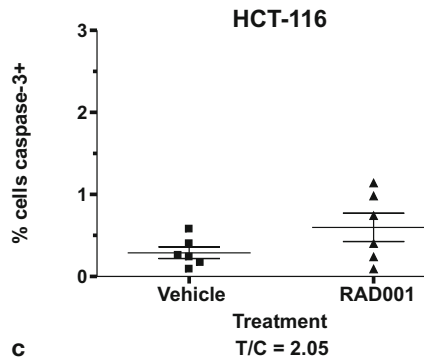
HCT-116
% cells caspase-3+
3
2
1
0
Vehicle
RAD001
Treatment
T/C = 2.05

c

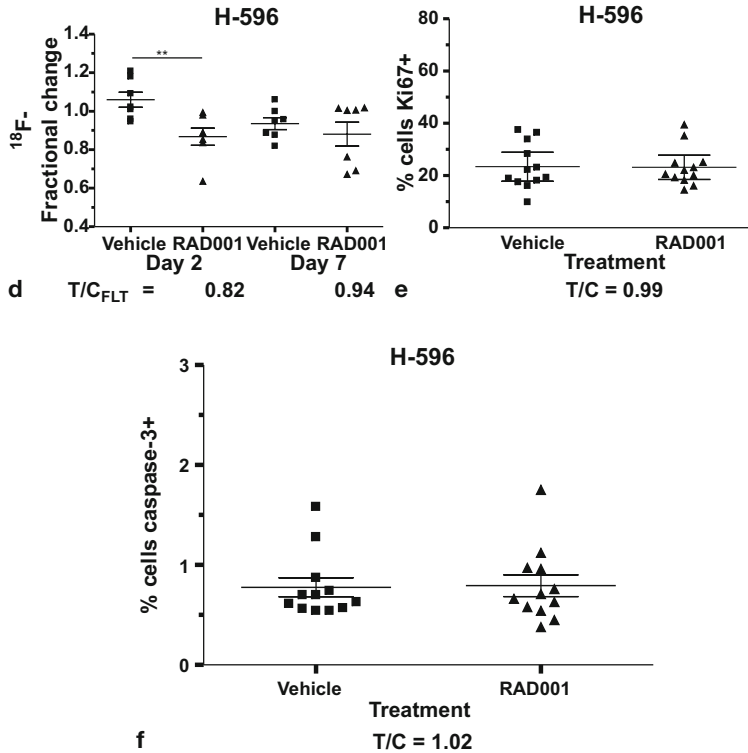

Fig. 10e–f. Effect of RAD001 on FLT uptake in two different tumour models and comparison with IHC measurements ex vivo. The results show the fractional change in FLT-NUV after 2–10 days daily treatment (10 mg/kg p.o. daily) and the associated T/C. In addition, for each model the IHC analysis of the Ki67 and apoptotic index is shown for each treatment group. For FLT, the results show the values for individual tumours and associated mean±SEM on respective days (significance assessed using a 2W-RM-ANOVA) and individual fractional changes and associated mean±SEM relative to baseline measurements (significance assessed using a two-tailed *t*-test). For IHC, the values for individual tumours and associated mean±SEM are shown for the respective endpoint

4 Conclusions

The basal IFP of a tumour is dependent both upon the individual tumour cells and the milieu in which it grows so that the type of host (e.g. mouse vs rat) can strongly affect the basal IFP, but not the site within an individual host. If one can draw a further conclusion from this relatively small study it would be that rat tumour cells in rats tend to have higher IFPs than mouse or human tumour cells grown in mice. With regard to drug response, there was some evidence that the basal IFP could also be a stratifier, since tumours with a higher IFP tended to show the best response to the compounds EPO906 and PTK787. However, these were not highly significant correlations (approximately $p = 0.05$), especially in comparison to the correlations found for the early fractional change in IFP (ΔIFP) and the eventual change in tumour volume (ΔTVol) for the compounds EPO906, Gemzar and PTK787 in the two orthotopic models of BN472 and RIF-1. Such data suggest that IFP changes could be a useful generic early-response marker for tumour response to therapy. However, these significant correlations were not evident in the ectopic models, except in the 1A9 model treated with EPO906, where there was a weaker correlation ($r = 0.3$, $p < 0.01$) but only when comparing late ΔIFP and ΔTVol. This may well reflect the different vascular architecture of ectopic and orthotopic tumours, as illustrated by a number of methods discussed in this report. DCE-MRI showed that the ectopic models were much better perfused on the rim than in the large, often necrotic portion of the tumour, and FDG-PET also showed very strikingly that viable cells and/or blood flow were rim-limited; of course this was confirmed ex vivo by H&E histology. In general, this suggests that only the well-vascularised tumour models clearly demonstrated a correlation between an early decrease in IFP and the eventual tumour response.

Consistent with the above hypothesis were the results obtained with EPO906 and PTK787, which showed that both basal IFP and the drug-induced changes in IFP were related to vascular permeability, blood flow and total blood volume. The precise relationship depended on the compound's mechanism of action. Thus, the cytotoxic anti-vascular agent caused large decreases in BVol and also appeared to reduce the mean vessel size, without significantly affecting vascular permeability

or blood flow, while the VEGF-R targeted agent reduced permeability and increased blood flow without affecting blood volume. Histological analysis also confirmed a trend showing reduced mean vessel width. Both compounds therefore caused the tumours to manifest examples of a normalisation of the vasculature, albeit in different ways, with the anti-angiogenic activity being associated, perhaps transiently, with an increase in blood flow, thus masking the expected primary effect of reducing vascular permeability.

The data obtained in the FDG-PET experiments with PTK787 and RAD001 could also be considered to support the notion that anti-angiogenic activity is associated with an increase in tumour blood flow. Despite significantly inhibiting BN472 tumour growth, PTK787 failed to significantly impact FDG uptake after 2 or 7 days, and a similar phenomenon was seen with RAD001 in the less sensitive tumour models where the growth-inhibitory effect of RAD001 is considered to be at the level of the endothelium. The reason for this may be that a drug-induced increase in blood flow could mask a change in the number of viable actively glycolytic cells, since the method could not distinguish between FDG (intra- or extracellular) or phosphorylated FDG. Indeed, EPO906, which did not affect tumour blood flow, caused a large and rapid decrease in FDG uptake by BN472 tumours. In sensitive models, RAD001 was also able to significantly decrease tumour FDG uptake.

To a certain extent, similar data have so far been obtained using the PET-proliferation marker of FLT. RAD001 caused small but consistent decreases in FLT uptake by H-596 tumours, but not in the less sensitive HCT-116 tumour, a result similar to that seen with FDG-PET; and EPO906 caused a rapid decrease in FLT uptake of RIF-1 tumours.

Thus to sum up. Tumour IFP, and especially drug-induced changes in IFP, reflect the tumour vascular architecture and may be used as a generic early marker of tumour response. In all models studied, significant tumour efficacy is always eventually associated with a decrease in IFP. Interestingly, the same cannot be said of other noninvasive imaging methods measuring various aspects of tumour vasculature, metabolism and proliferation. This is because a drug can induce many different responses in the tumour that are specific but also nonspecific to the mechanism of action. Therefore, a more generic marker of cell viability or vascular status is likely to be the better universal early-response marker

Table 4 Effect of different compound classes on minimally invasive parameters 2–3 days after treatment initiation

Compound	Molecular target	iAUEC	Ktrans	BVol	IFP	FDG	FLT
EPO906	Micro-tubules	1.03	0.82	0.7*	0.41*	0.54*	0.78*
PTK787	VEGF-R	0.80*	0.37*	0.97	0.64*	0.94	–
RAD001	mTOR	1.13	1.34	1.1	0.74	0.70* HS 1.02 LS	0.82*

The values shown reflect the average T/Cs (fractional change in parameter for compound-treated divided by vehicle-treated) determined in several different experiments across one or frequently two different tumour models (BN472, B16/BL6, RIF-1, H-596, HCT-116, KB-31), where *indicates there was a significant difference relative to vehicle. For RAD001 on FDG, two values are shown to reflect the very different behaviour in low- and high-sensitivity models

of successful therapy. Unfortunately, IFP measurements in the clinic are not always feasible because of the position of the tumour, patient agreement, or indeed the perception of the treating clinician. This is understandable, and it means we still await the development of a fast, safe, easy, noninvasive and robust method to measure a parameter that always changes in the same direction when there is a significant response of the tumour to therapy. Therefore, for now, the optimal early-response biomarker for a particular compound remains to be identified preclinically before clinical trials are in place, because, as Table 4 illustrates, a biomarker change is not always predictable.

References

Ferretti S, Allegrini PR, O'Reilly T, Schnell C, Stumm M, Wartmann M, Wood J and McSheehy PM (2005) Patupilone induced vascular disruption in orthotopic rodent tumor models detected by magnetic resonance imaging and interstitial fluid pressure. Clin Cancer Res 11:7773–7784

Jain RK (1994) Barriers to drug deliver in solid tumors. Sci Am 271:58–65

Lee L, Sharma S, Morgan B, Allegrini P, Schnell C, Brueggen J, Cozens R, Horsfield M, Guenther C, Steward WP, Drevs J, Lebwohl D, Wood J, McSheehy PM (2006) Biomarkers for assessment of pharmacologic activity for a vascular endothelial growth factor (VEGF) receptor inhibitor, PTK787/ZK 222584 (PTK/ZK): translation of biological activity in a mouse melanoma metastasis model to phase I studies in patients with advanced colorectal cancer with liver metastases. Cancer Chemother Pharmacol 57:761–71

Mankoff DA, Muzi M, Krohn KA (2003) Quantitative positron emission tomography imaging to measure tumor response to therapy: what is the best method? Mol Imaging Biol 5:281–285

McSheehy P, Allegrini P, Honer M, Ebenhan T, Ametaby S, Schubiger P, Schnell C, Stumm M, O'Reilly T, Lane H (2007) Monitoring the activity of the mTor pathway inhibitor RAD001 (everolimus) non-invasively by functional imaging. Targeted Oncol 2:130–131

Milosevic M, Fyles A, Hedley D, Pintilie M, Levin W, Manchul L, Hill R (2001) Interstitial fluid pressure predicts survival in patients with cervix cancer independent of clinical prognostic factors and tumor oxygen measurements. Cancer Res 61:6400–6405

Rudin M, McSheehy PM, Allegrini PR, Rausch M, Baumann D, Becquet M, Brecht K, Brueggen J, Ferretti S, Schaeffer F, Schnell C, Wood J (2005) PTK787 / ZK222584, a tyrosine kinase inhibitor of vascular endothelial growth factor receptor, reduces uptake of the contrast agent GdDOTA by murine orthotopic B16/BL6 melanoma tumors and inhibits their growth in vivo. NMR Biomed 18:308–321

Rutz HP (1999) A biophysical basis of enhanced interstitial fluid pressure in tumors. Med Hypotheses 53:526–529

Schnell CR, Stauffer F, Allegrini PR, O'Reilly T, McSheeny PMJ, Dartois C, Stumm M, Cozens R, Littlewood-Evans A, García-Echeverría C, Maira S-M (2008) Effects on the dual pan-class I PI3K/mTor inhibitor NVP-BEZ235 on the tumour vasculature: implications for clinical imaging. Cancer Res 68 (in press)

Taghian AG, Abi-Raad R, Assaad SI, Casty A, Ancukiewicz M, Yeh E, Molokhia P, Attia K, Sullivan T, Kuter I, Boucher Y, Powell SN (2005) Paclitaxel decreases the interstitial fluid pressure and improves oxygenation in breast cancers in patients treated with neoadjuvant chemotherapy: clinical implications. J Clin Oncol 23:1951–1961

Troprès I, Grimault S, Vaeth A, Grillon E, Julien C, Payen JF, Lamalle L, Décorps M (2001) Vessel size imaging. Magn Reson Med 45:397–408

Willett CG, Boucher Y, di Tomaso E, Duda DG, Munn LL, Tong RT, Chung DC, Sahani DV, Kalva SP, Kozin SV, Mino M, Cohen KS, Scadden DT, Hartford AC, Fischman AJ, Clark JW, Ryan DP, Zhu AX, Blaszkowsky LS, Chen HX, Shellito PC, Lauwers GY, Jain RK (2004) Direct evidence that the VEGF-specific antibody bevacizumab has antivascular effects in human rectal cancer. Nat Med 10:145–147